analytical chemistry

Article

Cite This: Anal. Chem. 2018, 90, 2954−2962

pubs.acs.org/ac

Organelle-Directed Staudinger Reaction Enabling Fluorescence-on Resolution of Mitochondrial Electropotentials via a Self-Immolative Charge Reversal Probe

Zhongwei Xue,[†] Rui Zhu,[†] Siyu Wang,[†] Jian Li,[†] Jiahuai Han,[‡] Jian Liu,*[,†,§] and Shoufa Han*[,†]

[†]Department of Chemical Biology, College of Chemistry and Chemical Engineering, State Key Laboratory for Physical Chemistry of Solid Surfaces, the Key Laboratory for Chemical Biology of Fujian Province, The MOE Key Laboratory of Spectrochemical Analysis and Instrumentation, and Innovation Center for Cell Signaling Network, and [‡]State Key Laboratory of Cellular Stress Biology, Innovation Center for Cell Signaling Network, School of Life Sciences, Xiamen University, Xiamen, 361005, China

[§]School of Pharmacy, Lanzhou University, Lanzhou, 73000, China

Supporting Information

ABSTRACT: Organelles often feature parameters pertinent to functions and yet responsive to biochemical stress. The electropotential across the mitochondrial membrane (ΔΨm) is a crucial mediator of cell fates. Herein we report a bioorthogonal reaction enabled fluorescence-on probing of ΔΨm alterations featuring anionic fluorescein-triphenylphosphonium diad (F-TPP), which is released via intramitochondria Staudinger reaction triggered self-immolation of *o*-azidomethylbenzoylated F-TPP. Compared to classical cationic mitochondria-specific dyes, F-TPP is hydrophilic and negatively charged. Effectively discerning ΔΨm changes upon diverse stress inducers, the organelle-directed bioorthogonal imaging strategy offers unprecedented choices to probe mitochondrial biology with functional molecules that are otherwise inaccessible via physiological organelle-probe affinity.

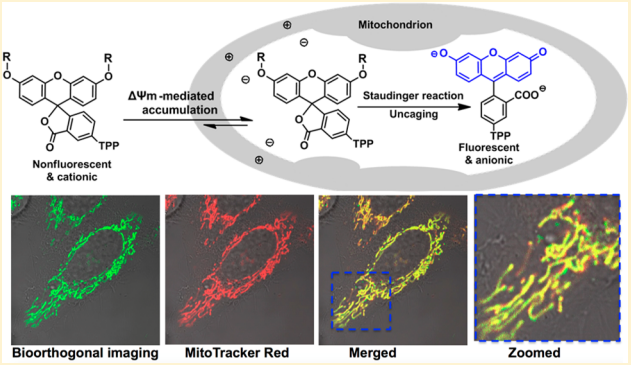

Cell fate is largely shaped by intracellular organelles that often display stress-responsive parameters critical for organelle activities. Mitochondria are bioenergetic and signaling organelles featuring negative electrical potentials across the inner membrane (ΔΨm).[1] Central to mitochondrial functionality, ΔΨm is essential for critical cellular events such as ATP resynthesis and cell proliferation.[2] Attenuated ΔΨm has been linked to autophagy, cell death, and multiple diseases such as Parkinson's disease.[3−6] Given the myriad roles of ΔΨm in cell physiology and diseases, it is imperative to discern ΔΨm status in live cells.

Lipophilic and cationic dyes, for example, rhodamine 123 and JC-1, concentrate in mitochondria driven by ΔΨm, and are often used to image mitochondria.[7,8] To date, ΔΨm alterations are largely examined by cationic probes of "always-on" fluorescence.[9] Herein we report the "signal-on" imaging of mitochondria with anionic and fluorescence F-TPP, which is generated from nonfluorescent ^{Az}F-TPP via intramitochondrial Staudinger reaction. ^{Az}F-TPP contains a core of *o*-azidomethylbenzoyl-fluorescein and a cationic TPP moiety. ^{Az}F-TPP accumulates in mitochondria driven by ΔΨm, and undergoes Staudinger reaction mediated self-immolation to give fluorescent F-TPP. Relative to classic cationic mito-tropic dyes, F-TPP is hydrophilic and negatively charged in alkaline mitochondrial lumen (pH 8; Scheme 1) and effectively discerns ΔΨm alteration in live cells.

EXPERIMENTAL PROCEDURE

Materials and Methods. Amytal, oligomycin, Mito-Tempo, carbonyl cyanide-*p*-trifluoromethoxyphenylhydrazone (FCCP), rotenone, and carbonyl cyanide *m*-chlorophenylhydrazone (CCCP) were purchased from Sigma. Mitotracker Red CMXRos, Hoechst 33342, JC-1, TMRM, and rhodamine 123 were purchased from Thermo Fisher. All other chemicals were obtained from Alfa-Aesar unless specified. Column chromatography was performed on silica gel (100−200 mesh). NMR spectra were recorded on a Bruker instrument using tetramethyl silane as the internal reference. Mass analysis was performed in Bruker En Apex ultra 7.0T FT-MS. Fluorescence spectra and UV−vis absorption spectra were recorded on a spectrofluorometer (SpectraMax M5, Molecular Device).

HeLa cells were obtained from American Type Culture Collection (ATCC). Cells were maintained in Dulbecco's modified Eagle's medium (DMEM), supplemented with 10%

Received: December 31, 2017
Accepted: January 29, 2018
Published: January 29, 2018

DOI: 10.1021/acs.analchem.7b05465
Anal. Chem. 2018, 90, 2954−2962

Scheme 1. Intramitochondrial Staudinger Reaction Mediated Fluorescence-on Imaging of Mitochondria[a]

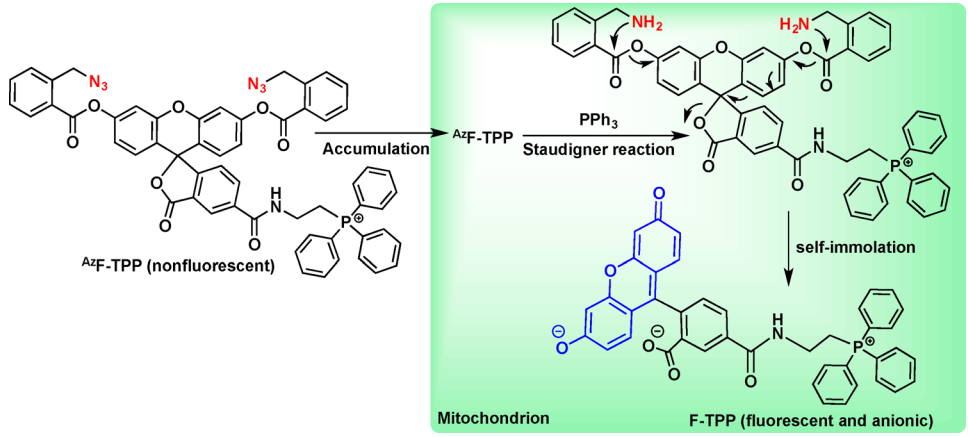

[a]Cationic ^{Az}F-TPP accumulates in mitochondria and undergoes tandem triphenylphosphine (PPh_3) mediated azide-reduction and self-immolation to give fluorescent and anionic F-TPP.

fetal bovine serum, 2 mM L-glutamine, 100 IU penicillin, and 100 mg/mL streptomycin at 37 °C in a humidified incubator containing 5% CO_2. Fluorescence spectra were performed on SpectraMax M5. Confocal fluorescence microscopic imaging was performed on Zeiss LSM 780 using the following filters: λ_{ex} = 405 nm and λ_{em} = 410−483 nm for Hoechst, λ_{ex} = 488 nm and λ_{em} = 499−553 nm for rhodamine 123, JC-1 and fluorescein, λ_{ex} = 565 nm and λ_{em} = 585−733 nm for TMRM and Mitotracker Red. The fluorescence of Mitotracker Red and hoechst in cells was respectively shown in red and blue in the figures while fluorescence of rhodamine 123 and fluorescein in cells was shown in green. Images of merged fluorescence were using Photoshop CS6. Quantitative imaging analysis was carried out on unprocessed images using ImageJ software. Graph was generated by GraphPad Prism5 and origin 8.0 software.

Flow cytometry analysis was performed on BD Fortessa, the fluorescence of TMRM was recorded by PE filter (569−601 nm) using excitation wavelength of 561 nm, while that of rhodamine 123, JC-1, and F-TPP were recorded by FITC filter (500−560 nm) using excitation wavelength of 488 nm. 10000 cells were gated under identical conditions, analyzed, and the data were processed by GraphPad Prism5.

Synthesis of ^{Az}F-TPP (Scheme S1, Supporting Information). To a flask containing DMF (25 mL) was added compound **1** (500 mg, 1.06 mmol), 2-aminoethyltriphenylphosphonium bromide (595 mg, 1.27 mmol), and K_2CO_3 (585 mg, 4.24 mmol). The reaction mixture was stirred at 50 °C for 3 h and then concentrated to remove DMF under vacuo. The residue was purified by flash column chromatography (CH_2Cl_2/HCl in CH_3OH (5%) = 10:1) to give F-TPP as a yellow powder (612 mg) in 87.2% yield. ^{1}H NMR (500 MHz, MeOD) δ 8.32 (d, J = 47.4 Hz, 1H), 8.15−8.03 (m, 1H), 7.97−7.82 (m, 10H), 7.82−7.70 (m, 6H), 7.26 (dd, J = 20.0, 6.3 Hz, 1H), 6.68 (dd, J = 14.5, 5.4 Hz, 4H), 6.58 (dd, J = 8.8, 2.1 Hz, 2H), 3.94−3.78 (m, 4H). ^{13}C-DEPT 135 NMR (126 MHz, MeOD) δ 135.03 (d, J = 2.9 Hz), 133.52 (d, J = 10.3 Hz), 130.24 (d, J = 12.8 Hz), 129.15 (s), 102.41 (s), 33.79 (s), 21.84 (d, J = 50.6 Hz). HRMS (ESI): Calcd $C_{41}H_{31}NO_6P^+$ [M^+], 664.1884; found, 664.1888.

2-(Azidomethyl)benzoic acid (160 mg, 0.90 mmol) and 3-thylvarbodiimide hydrochloride (EDC; 230 mg, 1.20 mmol) were added into a flask containing anhydrous pyridine (10 mL). The reaction mixture was allowed to stir at room temperature for 1 h, followed by addition of F-TPP (200 mg, 0.30 mmol) and *N*,*N*-dimethylaminopyridine (DMAP; 10 mg, 0.08 mmol) and then stirred at room temperature for 2 h. The mixture was concentrated to remove pyridine. The residue was extracted between CH_2Cl_2 (50 mL) and aqueous hydrochloride (50 mL, 1 M). The organic layer was dried over Na_2SO_4 and then concentrated. The resulting residue was purified by flash column chromatography (CH_2Cl_2/CH_3OH = 20:1) to afford ^{Az}F-TPP as a off-white powder (243 mg, 81.8%). ^{1}H NMR (500 MHz, $CDCl_3$) δ 10.26 (s, 1H), 8.61 (s, 1H), 8.54 (d, J = 8.1 Hz, 1H), 8.30−8.23 (m, 2H), 7.85 (dd, J = 12.9, 7.4 Hz, 6H), 7.79 (dd, J = 8.2, 6.5 Hz, 3H), 7.69 (ddd, J = 12.9, 6.5, 2.3 Hz, 6H), 7.65 (dd, J = 7.5, 1.0 Hz, 2H), 7.59 (d, J = 7.5 Hz, 2H), 7.50 (t, J = 7.6 Hz, 2H), 7.27 (s, 1H), 7.26 (s, 2H), 6.97 (dd, J = 8.7, 2.2 Hz, 2H), 6.89 (d, J = 8.7 Hz, 2H), 4.88 (s, 4H), 4.01 (s, 4H). ^{13}C-DEPT 135 NMR (126 MHz, $CDCl_3$) δ 135.17 (d, J = 3.0 Hz), 134.74 (s), 133.65 (s), 133.57 (d, J = 10.3 Hz), 131.67 (s), 130.50 (d, J = 12.7 Hz), 129.81 (s), 129.00 (s), 128.25 (s), 125.46 (s), 124.15 (s), 117.89 (s), 110.59 (s), 52.99 (s), 33.89 (s), 22.63 (d, J = 49.4 Hz). HRMS (ESI): Calcd $C_{57}H_{41}N_7O_8P^+$ [M^+], 982.2749; found, 982.2743.

Synthesis of ^{Az}F (Scheme S2, Supporting Information). 2-(Azidomethyl)benzoic acid (320 mg, 1.80 mmol) and EDC (460 mg, 2.40 mmol) were to a flask containing anhydrous pyridine (10 mL). The reaction mixture was allowed to stir at room temperature for 1 h and then added fluorescein (200 mg, 0.60 mmol) and DMAP (10 mg, 0.08 mmol). The mixture was stirred for 2 h and then concentrated. The residue was dissolved with CH_2Cl_2 (50 mL) washed by aqueous hydrochloride (50 mL, 1 M) and then dried over Na_2SO_4. The organic solution was concentrated and the resulting residue was purified by flash column chromatography (PE/DCM = 1:1) to give ^{Az}F as the desired product (320 mg) in 82.1% yield. ^{1}H NMR (500 MHz, $CDCl_3$) δ 8.31−8.21 (m, 2H), 8.06 (d, J = 7.6 Hz, 1H), 7.71 (tt, J = 6.0, 3.0 Hz, 1H), 7.69−7.63 (m, 3H), 7.62−7.55 (m, 2H), 7.50 (t, J = 7.6 Hz, 2H), 7.24 (dd, J = 8.0, 4.9 Hz, 2H), 6.96 (dt, J = 7.7, 3.8 Hz, 2H), 6.92 (d, J = 8.7 Hz, 2H), 4.87 (s, 4H). ^{13}C-DEPT 135 NMR (126 MHz, $CDCl_3$) δ 135.28, 133.71, 131.67, 130.04, 129.94, 129.04, 128.30, 125.20, 123.99, 117.87, 110.56, 53.01. LRMS (ESI): Calcd for $C_{36}H_{23}N_6O_7^+$ [M + H^+], 651.2; found, 651.2.

Synthesis of PPh_3-TPP (Scheme S3, Supporting Information). (3-Aminopropyl)triphenylphosphonium bromide (376 mg,

DOI: 10.1021/acs.analchem.7b05465
Anal. Chem. 2018, 90, 2954−2962

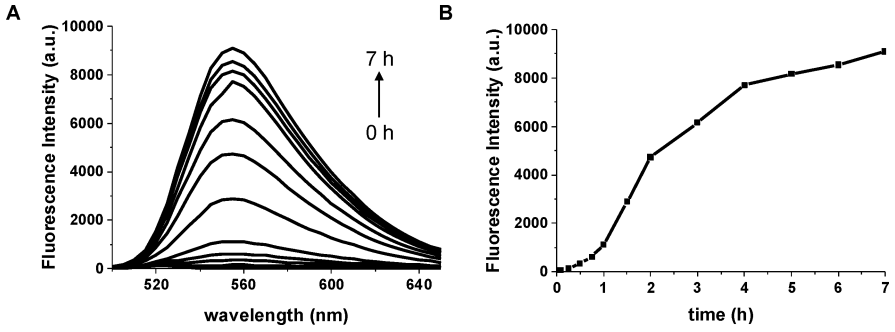

Figure 1. Staudinger reaction mediated fluorogenic formation of F-TPP from ^{Az}F-TPP. (A) Fluorescence emission of buffer (pH 8.0) spiked with ^{Az}F-TPP and PPh_3 at indicated time points postincubation (λ_{ex} = 520 nm). (B) Plot of fluorescence intensity at 560 nm over incubation time.

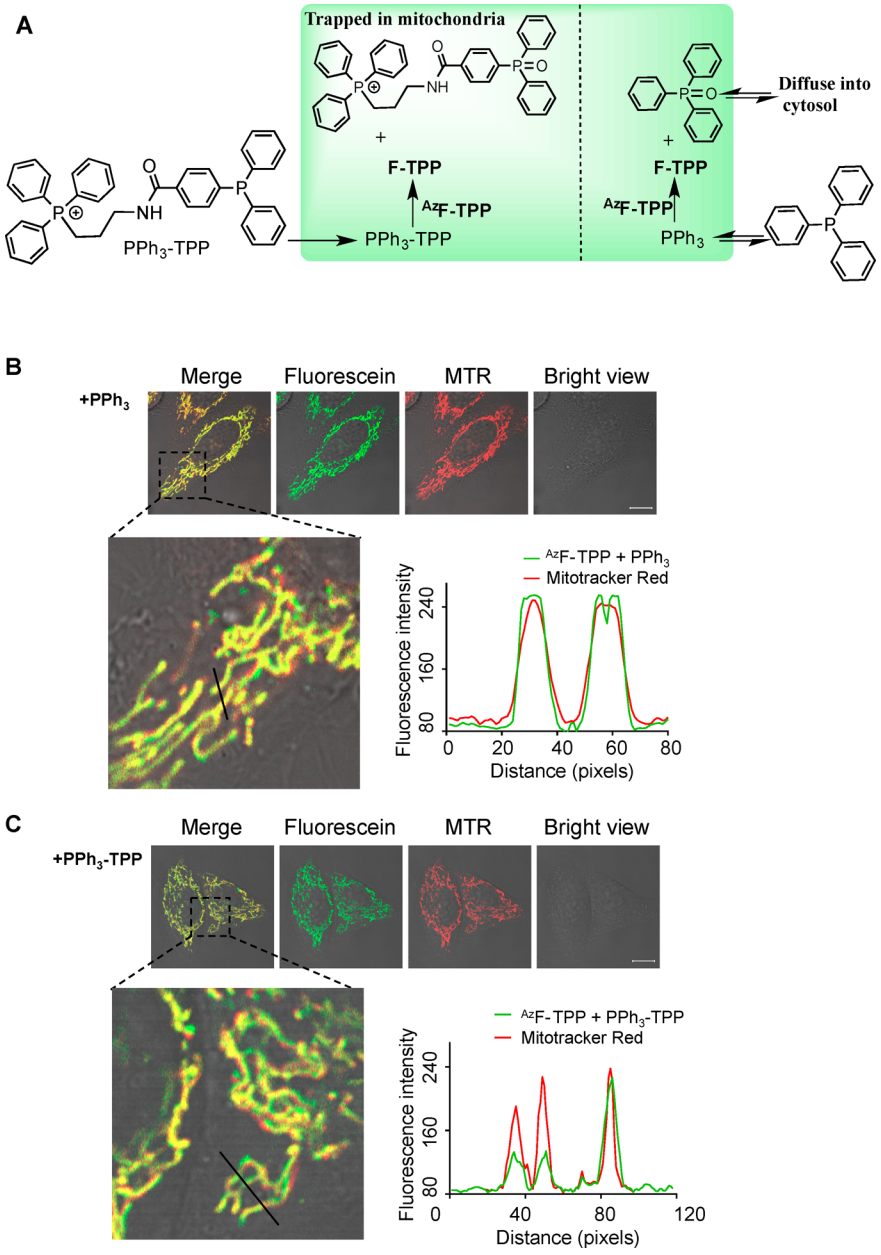

Figure 2. Staudinger reaction enabled selective imaging of mitochondria. (A) Schematic for Staudinger reaction between mitochondria-trapped ^{Az}F-TPP with diffuable PPh_3 over mitochondria-trapped PPh_3-TPP. HeLa cells cultivated with Mitotracker Red (MTR) and ^{Az}F-TPP were treated with PPh_3 (B) or PPh_3-TPP_3 (C) and then analyzed by confocal fluorescence microscopy. Plots show fluorescence of Mitotracker Red and F-TPP measured along the lines shown in zoomed images, which reveal colocalization of F-TPP with MTR. Scale bars, 10 μm.

DOI: 10.1021/acs.analchem.7b05465
Anal. Chem. 2018, 90, 2954−2962

1.18 mmol) was added in one portion to the solution of 4-(diphenylphosphenyl)benzoic acid (200 mg, 0.65 mmol), HOBT (106 mg, 0.78 mmol), EDC (150 mg, 0.78 mmol), and DIPEA (253 mg, 1.96) in dimethylfomaldehyde (DMF; 6 mL), which is maintained on ice and protected under nitrogen. The mixture was allowed to warm to room temperature and further stirred overnight. The reaction solution was concentrated and then extracted twice with EtOAc (50 mL). The combined organic phase was washed with water (100 mL), saturated brine (100 mL), and then concentrated. The residue was purified by silica gel flash chromatography (DCM/CH_3OH = 20:1) to give PPh_3-TPP as a white solid (260 mg, 0.43 mmol, 67% yield). ^1H NMR (500 MHz, $CDCl_3$) δ 9.23 (t, J = 6.0 Hz, 1H), 8.17 (dd, J = 8.3, 1.2 Hz, 2H), 7.72 (ddd, J = 8.2, 6.0, 5.2 Hz, 9H), 7.66−7.56 (m, 6H), 7.39−7.25 (m, 11H), 3.89−3.79 (m, 2H), 3.79−3.67 (m, 2H), 1.99 (ddd, J = 20.1, 11.3, 5.8 Hz, 2H). ^{13}C NMR (126 MHz, $CDCl_3$) δ 167.42 (s), 141.54 (d, J = 12.7 Hz), 136.58 (d, J = 10.5 Hz), 135.12 (d, J = 3.0 Hz), 133.94 (d, J = 19.7 Hz), 133.51 (d, J = 35.6 Hz), 133.48 (d, J = 9.9 Hz), 130.56 (d, J = 12.5 Hz), 128.99 (s), 128.96 (d, J = 52.8 Hz), 128.64 (d, J = 7.2 Hz), 127.90 (d, J = 6.7 Hz), 118.28 (d, J = 86.2 Hz), 39.28 (d, J = 16.6 Hz), 22.50 (d, J = 3.7 Hz), 20.99 (d, J = 52.0 Hz). LR-MS (ESI): $C_{40}H_{36}NOP_2^+$ [M^+] Calcd, 608.2; found, 608.3.

In Vitro Generation of F-TPP from ^{Az}F-TPP. The stock solution of PPh_3 in DMF was spiked into Tri-HCl buffer (200 mM, pH 8.0) containing ^{Az}F-TPP (10 mM) to a final concentration of 25 mM. The solution was maintained at room temperature. An aliquots of the solution was diluted 10 folds and then assayed for fluorescence emission at 0, 5, 15, 30, and 45 min and 1, 1.5, 2, 3, 4, 5, 6, and 7 h postincubation. The solution was analyzed by mass spectrometry at 7 h after incubation.

Selectivity of ^{Az}F-TPP toward PPh_3 over Biological Reductants. To ^{Az}F-TPP (10 mM) in Tris-HCl buffer (pH 8, 100 mM, 40% DMF) were supplemented with dithiothreitol (DTT) (25 mM), cysteine (25 mM), GSH (25 mM), Mito-Tempo (0.6 mM), PPh_3 (25 mM) or no addition. Fluorescence emission of the samples (Ex: 520 nm, Em: 560 nm) were monitored and recorded as a function of incubation time (0, 10, 30, 60, 90, 240, and 420 min).

Imaging of Mitochondria with ΔΨm-Directed Staudinger Reaction. HeLa cells cultivated with Mitotracker Red

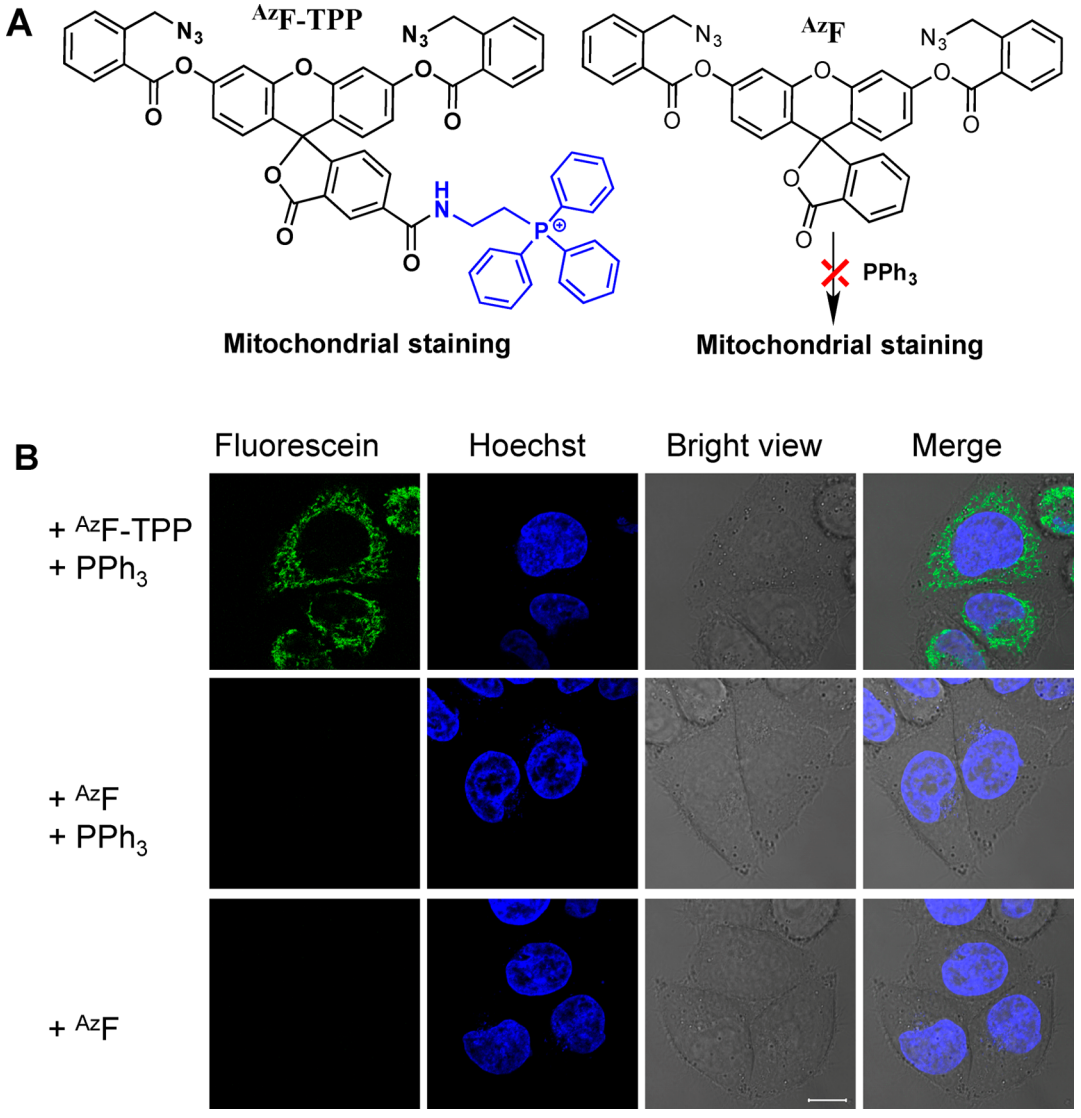

Figure 3. Dependence of ^{Az}F-TPP on Staudinger reaction mediated mitochondrial imaging. (A) Chemical structures of ^{Az}F-TPP and ^{Az}F. (B) Confocal microscopic images of HeLa cells cultivated with ^{Az}F, ^{Az}F/PPh_3, or ^{Az}F-TPP/PPh_3. Scale bar, 10 μm.

DOI: 10.1021/acs.analchem.7b05465
Anal. Chem. 2018, 90, 2954−2962

(MTR, 100 nM) and ^{Az}F-TPP (5 μM) were treated with PPh_3 (8 μM) or PPh_3-TPP (8 μM) for 1 h and then analyzed by confocal fluorescence microscopy. Plots of fluorescence of Mitotracker Red, and F-TPP were measured along the lines shown in zoomed images by ImageJ.

Incapability of Mitochondria to Uptake F-TPP. HeLa cells were stained by ^{Az}F-TPP (5 μM) or F-TPP (5 μM) together with PPh_3 (8 μM) for 1 h and then washed by fresh DMEM for 3 times. Cells were analyzed by confocal fluorescence microscopy.

Phosphine Dependent Staining of Mitochondria. HeLa cells were respectively cultivated with ^{Az}F-TPP (5 μM) together with PPh_3 (8 μM), PPh_3-TPP (8 μM), or no addition for 1 h and then rinsed with fresh DMEM for 3 times. Cells were analyzed by confocal fluorescence microscopy.

^{Az}F-TPP Dependent Staining of Mitochondria. HeLa cells were cultured in DMEM containing ^{Az}F (5 μM), ^{Az}F (5 μM)/PPh_3 (8 μM) or ^{Az}F-TPP (5 μM)/PPh_3 (8 μM) for 1 h and then cells were rinsed by fresh DMEM for 3 times before cofocal fluorescence microscopic imaging.

Comparison on Temporal Retention of F-TPP with Mitochondria-Specific Dyes. HeLa cells cultivated with rhodamine 123 (1 μM), JC-1 (5 mg/mL), and TMRM (100 nM) for 10 min or ^{Az}F-TPP (5 μM)/PPh_3 (8 μM) for 1 h, and then cells were washed by fresh DMEM for 3 times and cultured in DMEM for 0, 24, and 48 h. The cells were analyzed by confocal fluorescence microscopy.

Comparison on ΔΨm-Dependent F-TPP Retention in Mitochondria with Mitochondria-Specific Dyes. HeLa cells were cultured in DMEM with or without 20 μM CCCP for 24 h and then cells were stained by rhodamine 123 (1 μM), JC-1 (5 mg/mL), and TMRM (100 nM) for 10 min or ^{Az}F-TPP (5 μM)/PPh_3 (8 μM) for 1 h. Cells were washed with fresh DMEM for 3 times before confocal fluorescence microscopic imaging.

For CCCP-dose dependent retention, HeLa cells were cultured in DMEM contained various doses of CCCP (0, 2, 4, 8, 10, and 20 μM) for 24 h and then cells were stained by rhodamine 123 (1 μM), JC-1 (5 mg/mL), and TMRM (100 nM) for 10 min or ^{Az}F-TPP (5 μM)/PPh_3 (8 μM) for 1 h. Cells were washed with fresh DMEM for 3 times and analyzed by flow cytometry.

Cytotoxicity Analysis. The cytotoxicity of ^{Az}F-TPP and PPh_3 was evaluated on HeLa cells. Cells were cultured in 48 well cell culture plate with medium containing ^{Az}F-TPP (5 μM) and PPh_3 (0, 2, 4, 8, and 16 μM) for 1 h and washed with prewarmed DMEM for 3 times, then incubated with fresh DMEM for 12, 24, and 48 h. The cell number and cell viability were determined by MTT assay. The cells were cultured in 48 well cell culture plate with medium containing PPh_3 (8 μM) and ^{Az}F-TPP (0, 1, 2, 5, and 10 μM) for 1 h and washed with prewarmed DMEM for 3 times, then incubated with fresh DMEM for 12, 24, and 48 h. The cell number and cell viability were determined by MTT assay.

Photostability of F-TPP. HeLa cells were cultivated with PPh_3 (8 μM) and ^{Az}F-TPP (5 μM) for 1 h and washed with prewarmed DMEM for 3 times, then cells were illuminated for 1 h and scanned for 12 times per 5 min with a confocal

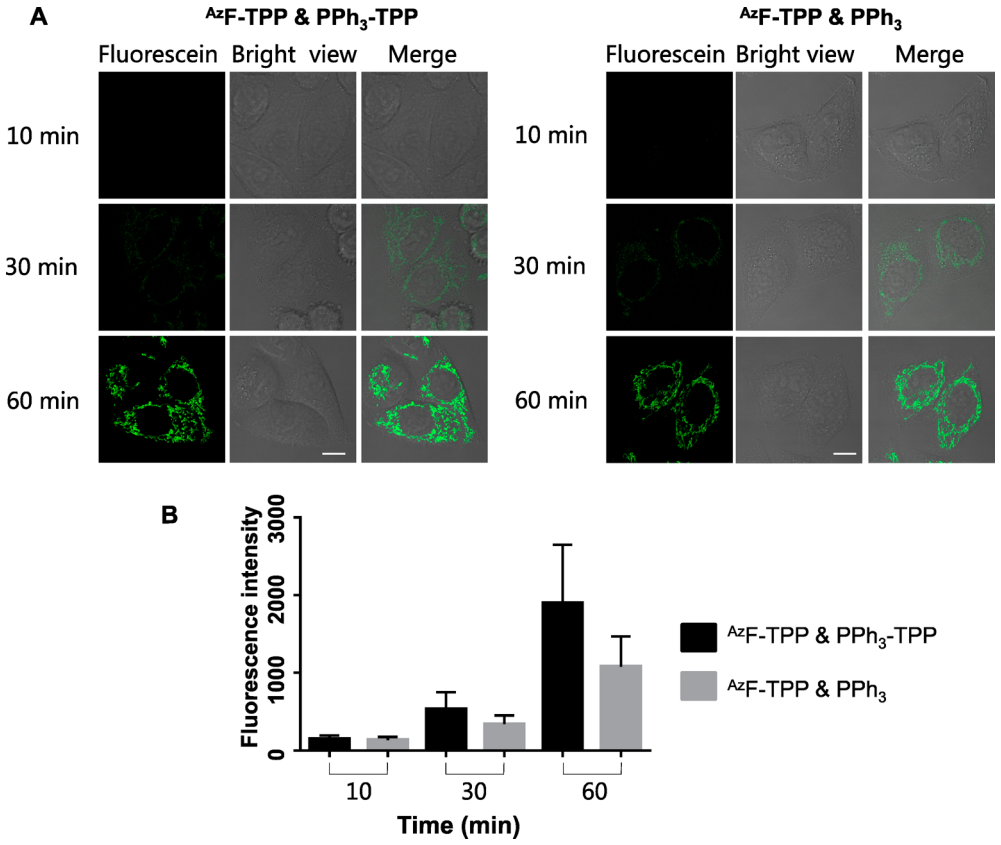

Figure 4. Comparison of PPh_3 with PPh_3-TPP on fluorogenic mitochondria staining with ^{Az}F-TPP. HeLa cells were cultivated with ^{Az}F-TPP/PPh_3-TPP or ^{Az}F-TPP/PPh_3 and then analyzed by confocal microscopy (A) and flow cytometry (B) at indicated time points postincubation. Scale bars, 10 μm. Error bars represent standard deviation of 10000 cells.

DOI: 10.1021/acs.analchem.7b05465
Anal. Chem. 2018, 90, 2954−2962

fluorescence microscope. The fluorescence intensity of cells was calculated by ImageJ.

Effects of Biochemical Reagents on ΔΨm. HeLa cells were cultured with FCCP (5 μM), oligomycin (40 μM), rotenone (50 μM), amytal (5 mM), Mito-Tempo (250 μM), or no addition for varied periods of time (0, 4, 8, 16, 24 h), then cells were washed by prewarmed DMEM and stained with rhodamine 123 (1 μM), JC-1 (5 mg/mL), and TMRM (100 nM) for 10 min or ^{Az}F-TPP (5 μM)/PPh_3 (8 μM) for 1 h. Cells were analyzed by flow cytometry for intracellular fluorescence. Error bars represent standard deviation of 10000 cells.

RESULTS AND DISCUSSION

Staudinger Reaction Mediated Fluorogenic Genesis of ^{Az}F-TPP. Given the popularity of mitotropic "always-on" cationic dyes, we sought to explore an alternative approach to probe mitochondria with an anionic "turn-on" sensor. Staudinger reaction utilizes the reducing power of phosphines to convert azides into amines,[10,11] and later was adapted into a bioorthogonal reaction to label azides in biological systems.[12−14] *o*-(Azidomethyl)benzoyl moiety is a hydroxyl protecting group[15] and has been used as the responsive domain in a chemodosimeter.[16] Inspired by these findings, ^{Az}F-TPP was fabricated to contain a ΔΨm-responsive TPP moiety widely used to ferry various cargoes into mitochondria[17−19] and a fluorogen of *o*-(azidomethyl)benzoyl-fluorescein, which is anticipated to undergo Staudinger reaction mediated unmasking to give F-TPP (Scheme 1).

To assess Staudinger reaction mediated fluorescence activation, the reaction of nonfluorescent ^{Az}F-TPP with PPh_3 in aqueous medium was monitored by fluorometry. We observed genesis of fluorescence peaked at 560 nm, which intensified over time (Figure 1), indicating Staudinger reaction-triggered formation of F-TPP from ^{Az}F-TPP. In addition, high resolution mass spectrometry analysis of the reaction solution revealed a major peak located at 664.1888, which corresponds to F-TPP (664.1884; Figure S1, Supporting Information). These results clearly show the occurrence of Staudinger reaction mediated cleavage of *o*-(azidomethyl)benzoyl group of ^{Az}F-TPP to give F-TPP (Scheme 1).

Imaging of Mitochondria via Organelle-Directed Staudinger Reaction. We first incubated HeLa cells with in vitro synthesized F-TPP. The absence of F-TPP fluorescence inside cells shows the incapability of mitochondria to uptake anionic F-TPP (Figure S2, SI), which is consistent with ΔΨm-driven accumulation of cationic dyes in mitochondria. To ascertain the feasibility of Staudinger reaction-mediated mitochondria imaging, HeLa cells were cultivated with ^{Az}F-TPP in the presence of triphenylphosphine (PPh_3), TPP-labeled PPh_3 (PPh_3-TPP), or no addition. Punctate fluorescein signals were observed in PPh_3 or PPh_3-TPP-treated cells whereas no signals could be identified in cells cultured with ^{Az}F-TPP alone

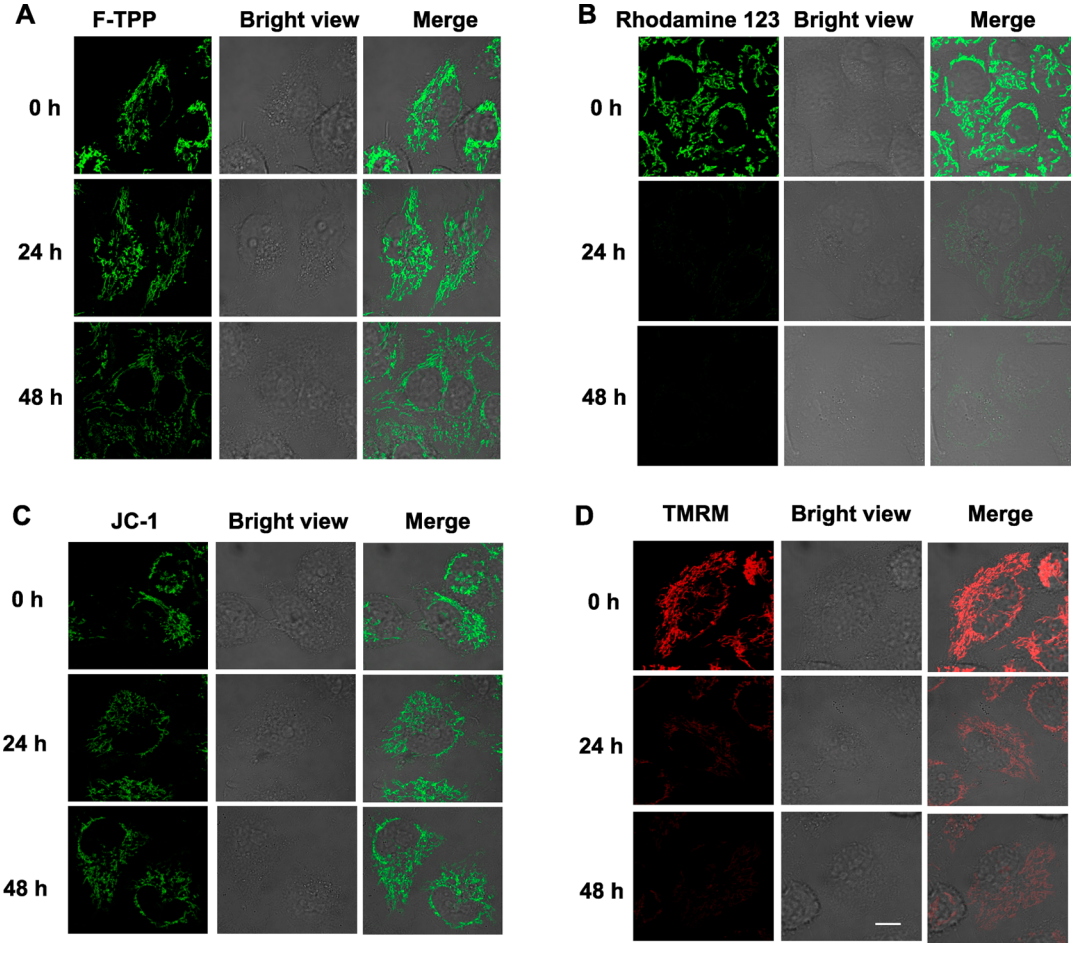

Figure 5. Retention of F-TPP in mitochondria as compared to commercial mitochondria-specific dyes. HeLa cell prestained with ^{Az}F-TPP/PPh_3 (A), rhodamine 123 (B), JC-1 (C), or TMRM (D) were maintained in fresh medium and analyzed for intracellular fluorescence over time by confocal fluorescence microscopy. Scale bars, 10 μm.

DOI: 10.1021/acs.analchem.7b05465
Anal. Chem. 2018, 90, 2954−2962

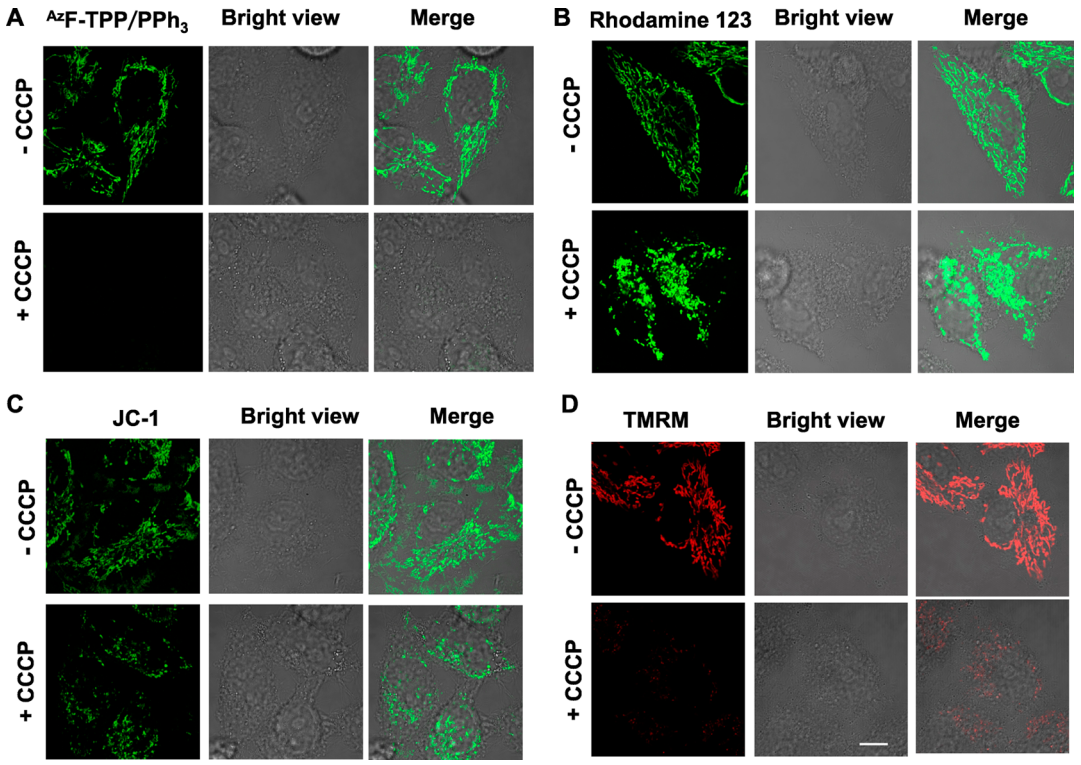

Figure 6. Comparison on detection of ΔΨm alterations with intramitochondrial Staudinger reaction with commercial mitochondria-specific dyes. HeLa cells were cultured with CCCP and then stained with ^{Az}F-TPP/PPh$_3$ (A) rhodamine 123 (B), JC-1 (C), or TMRM (D) and then visualized by confocal fluorescence microscopy analysis. Scale bar, 10 μm.

(Figure 2, Figure S3, Supporting Information), proving Staudinger reaction triggered "turn-on" fluorescence in cells. Furthermore, the intracellular F-TPP signals colocalized with Mitotracker Red (MTR) (Figure 2) specific for mitochondria, with Pearson's coefficient of 0.832 for PPh$_3$-TPP and 0.812 for PPh$_3$, proving selectivity of Staudinger reaction mediated mitochondria staining. Given the incapability of anionic F-TPP to target mitochondria, these results demonstrate the applicability of Staudinger reaction-triggered with in situ generated F-TPP for selective imaging of mitochondria.

^{Az}F is a structural analogue of ^{Az}F-TPP and lacks the TPP moiety (Figure 3A). No fluorescence was observed in cells costained with PPh$_3$-TPP and ^{Az}F (Figure 3B), proving the critical role of TPP moiety of ^{Az}F-TPP for mitochondria-directed Staudinger reaction. We performed time course monitoring on fluorescence intensities in cells treated PPh$_3$ over PPh$_3$-TPP in the presence of ^{Az}F-TPP. Comparable levels of intracellular fluorescence were identified in these two cell populations as determined by confocal microscopy (Figure 4A) and flow cytometry (Figure 4B), showing that PPh$_3$ diffused into mitochondria and converted ^{Az}F-TPP to give F-TPP with efficiency close to PPh$_3$-TPP. To minimize detrimental effects of exogenous species accumulated on mitochondrial health, PPh$_3$ is beneficial over PPh$_3$-TPP for Staudinger reaction mediated bioimaging owing to the ability of PPh$_3$ and the oxidized product (triphenylphosphine oxide) to diffuse out of mitochondria.

Shown to selectively illuminate mitochondria, we next investigated the temporal stability of Staudinger reaction enabled mitochondria imaging. HeLa cells stained with ^{Az}F-TPP/PPh$_3$ or commercial mito-probes were maintained in fresh media. Time course analysis showed that the signals of F-TPP and JC-1 remained intensive in cells after 48-h incubation (Figure 5A,C), whereas rhodamine 123 and tetramethylrhodamine methyl ester (TMRM) were largely dissipated (Figure 5B,D). Retention of anionic F-TPP is likely owing to mitochondrial inner membrane impermeable hydrophilic species.[8] In addition, no apparent cytotoxicity of ^{Az}F-TPP/PPh$_3$ was observed in HeLa cells (Figures S4 and S5, Supporting Information), which, together with effective retention of F-TPP in mitochondria, indicate the practical utility of Staudinger reaction mediated mitochondria imaging.

Probing Altered Ψm by Intramitochondrial Staudinger Reaction. We proceeded to determine the correlation of mitochondria-targeted Staudinger reaction with ΔΨm. HeLa cells were incubated with carbonyl cyanide *m*-chlorophenylhydrazone (CCCP) and then further stained with commercial mito-probes or ^{Az}F-TPP/PPh$_3$. CCCP is an ionphore effectively suppresses ΔΨm.[20,21] Relative to CCCP-free cells, obvious decreases of F-TPP and TMRM were identified in CCCP-spiked cells, whereas mitochondrial accumulation of rhodamine 123 is much less affected by CCCP (Figure 6). Consistently, flow cytometry analysis revealed CCCP-dose dependent attenuation of F-TPP and TMRM over rhodamine 123 (Figure S6, Supporting Information), showing the efficacy of Staudinger reaction enabled imaging of ΔΨm. The superior retention of F-TPP/JC-1 over TMRM and the sensitive detection of Ψm changes by F-TPP/TMRM over rhodamine 123 show that these probes are of distinct characters suitable for mitochondrial positioning or ΔΨm changes.

Historically, distinct methods have been developed to detect altered ΔΨm including intraorganelle Click chemistry based mass spectrometry,[9] the hetero-organelle partitioned sensors,[22,23] or fluorophores with potential-responsive properties.[24,25] In addition, ΔΨm manipulation has been achieved using photochemistry or metal catalysis.[26,27] In line with these

DOI: 10.1021/acs.analchem.7b05465
Anal. Chem. 2018, 90, 2954−2962

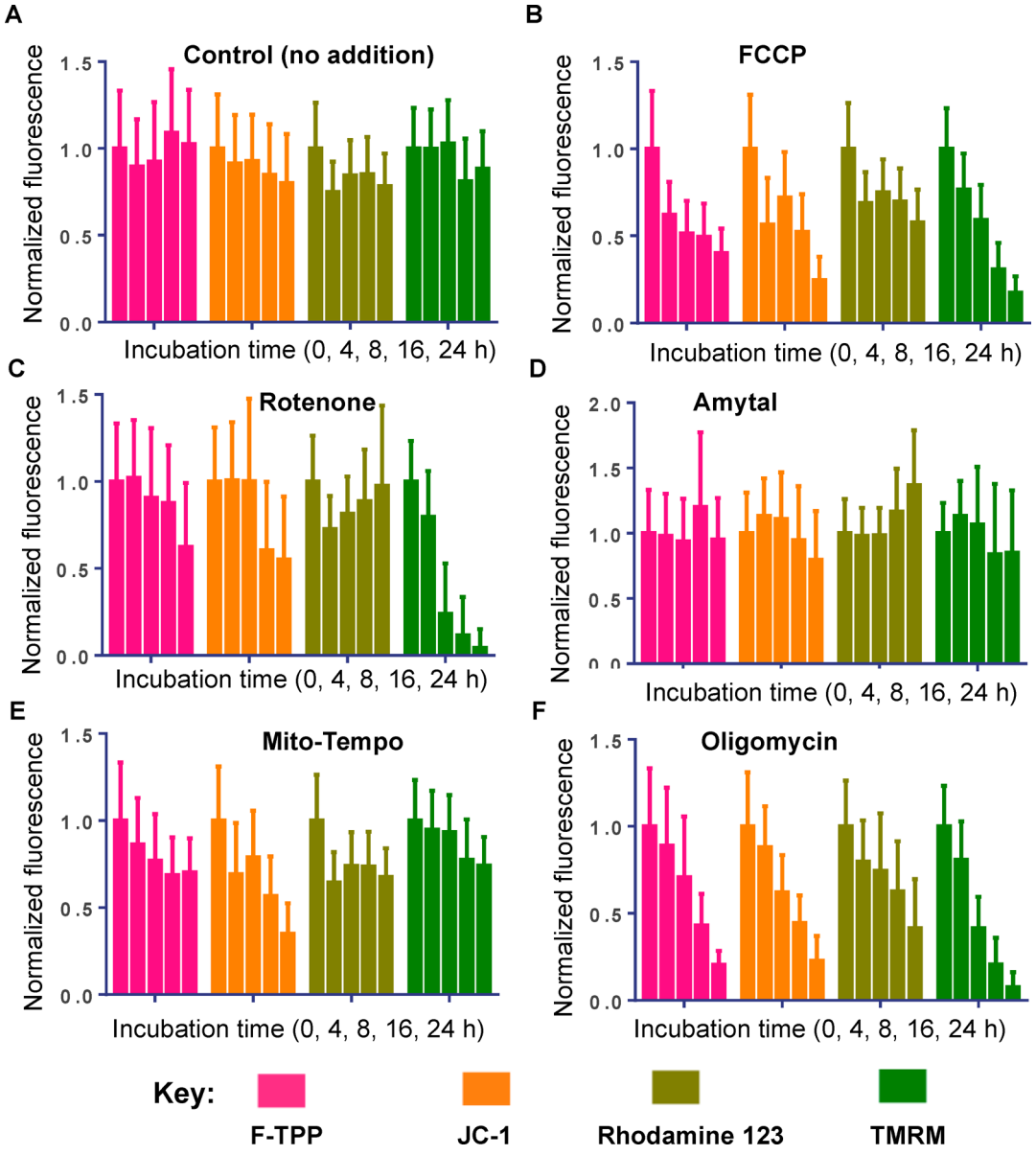

Figure 7. Effects of biochemical reagents on ΔΨm detected by intramitochondrial Staudinger reaction. HeLa cells were cultured with no addition (A), FCCP (5 μM) (B), rotenone (50 μM) (C), amytal (5 mM) (D), Mito-Tempo (250 μM) (E), or oligomycin (40 μM) (F), respectively, for varied periods of time (0, 4, 8, 16, and 24 h), stained with ^{Az}F-TPP/PPh$_3$, JC-1, rhodamine 123, or TMRM, and then analyzed by flow cytometry for intracellular fluorescence. Error bars represent standard deviation of 10000 cells.

approaches, this work developed a simplified method for facile fluorescence-on imaging of ΔΨm alteration by organelle-directed Staudinger reaction in living cells.

As dynamic organelles, mitochondria undergo ΔΨm changes upon biochemical stress.[28] Hence, HeLa cells were incubated with oligomycin, amytal, oligomycin, Mito-Tempo, retenone, or carboxyl cyanide-*p*-trifluoromethoxy-phenyl-hydrazone (FCCP), and then stained with ^{Az}F-TPP/PPh$_3$ or commercial mito-probes. Flow cytometry analysis shows that dramatic attenuation of ΔΨm is observed in FCCP-treated cells upon prolonged incubation as measured by decreased levels of F-TPP, JC-1, TMRM or rhodamine 123 within cells (Figure 7A,B), which is consistent with the roles of FCCP to dissipate ΔΨm.[29] Amytal and retenone inhibit mitochondria respiration by interfering NADH oxidation while oligomycin is an antibiotic blocking ATPase activity and oxidative phosphorylation.[30−32] Mito-Tempo is an antioxidant scavenging superoxide and alkyl radicals.[33] Despite indicator-specific variations in rotenone-spiked cells (Figure 7C), amytal, and Mito-Tempo exhibit no obvious or moderate effects on ΔΨm (Figure 7D,E), whereas oligomycin markedly attenuates ΔΨm over time as judged by four distinct mito-specific imaging reagents (Figure 7F). Oligomycin has been documented to inhibit oxidative phosphorylation and consequently hyperpolarizes mitochondria,[34] and this discrepancy to the observed mitochondrial depolarization by oligomycin (Figure 7F) is largely due to elongated incubation, whereby oligomycin inhibits ATP synthase and eventually causes cellular energy crisis. With the differential effects of mitochondria-targeted reagents on ΔΨm identified, these findings show the capability of Staudinger reaction mediated imaging to detect ΔΨm alterations under various biochemical stress.

Given the crucial roles of mitochondria in cancers,[35] mitochondria-targeting agents capable of disrupting mitochondria

DOI: 10.1021/acs.analchem.7b05465
Anal. Chem. 2018, 90, 2954−2962

functions have recently emerged as potential anticancer therapeutics.[36−41] The demonstrated use of the bioorthogonal imaging to detect ΔΨm changes suggests its potentials to evaluate mitochondria-interfering therapeutics in live cells.

CONCLUSIONS

Chemical tools are of use to probe organelle status in biology and diseases, such as ΔΨm alterations critical for diverse cellular events. Alternative to classical mitotropic cationic dyes, we present a bioorthogonal strategy for fluorogenic imaging of mitochondria with anionic F-TPP, which is decaged by intramitochondrial Staudinger reaction triggered self-immolation of nonfluorescent ^{Az}F-TPP. Effectively detecting stress-pertinent ΔΨm alterations, this organelle-directed bioorthogonal imaging strategy offers a practical route to interrogate mitochondria with functional molecules otherwise inaccessible via natural organelle-probe affinity.

ASSOCIATED CONTENT

Supporting Information

Supporting Information on . The Supporting Information is available free of charge on the ACS Publications website at DOI: 10.1021/acs.analchem.7b05465.

Spectral analysis of the new compounds, flow cytometry cell analysis, cell fluorescence analysis, cell cytotoxicity, photostability of F-TPP, and selectivity of ^{Az}F-TPP toward PPh_3 over biological thiols (PDF).

AUTHOR INFORMATION

Corresponding Authors

*E-mail: shoufa@xmu.edu.cn.

*E-mail: jianliu@lzu.edu.cn. Fax: +865922181728.

ORCID

Jian Liu: 0000-0002-6879-0614

Shoufa Han: 0000-0002-2057-0559

Notes

The authors declare no competing financial interest.

ACKNOWLEDGMENTS

This work was supported by grants from NSF China (21775130, 21572189), and the Fundamental Research Funds for the Central Universities (207201 60052, 20720150047), Xiamen University; Dr J. Han was supported by grants from NSF China (91429301, 31420103910, 31330047, 31221065), the National Scientific and Technological Major Project (2013ZX10002-002), the Hi-Tech Research and Development Program of China (863program; 2012AA02A201); Dr. J. Liu was supported by grant from NSF China (21602185).

REFERENCES

(1) Sherratt, H. S. *Rev. Neurol.* **1991**, *147*, 417−430.

(2) Friedman, J. R.; Nunnari, J. *Nature* **2014**, *505*, 335−343.

(3) Green, D. R.; Galluzzi, L.; Kroemer, G. *Science* **2011**, *333*, 1109−1112.

(4) Kamp, D. W.; Shacter, E.; Weitzman, S. A. *Oncology* **2011**, *25*, 400−410.

(5) McCoy, M. K.; Cookson, M. R. *Antioxid. Redox Signaling* **2012**, *16*, 869−882.

(6) Vyas, S.; Zaganjor, E.; Haigis, M. C. *Cell* **2016**, *166*, 555−566.

(7) Chazotte, B. *Cold Spring Harb. Protoc.* **2012**, *2012*, 892−894.

(8) Wisnovsky, S.; Lei, E. K.; Jean, S. R.; Kelley, S. O. *Cell Chem. Biol.* **2016**, *23*, 917−927.

(9) Logan, A.; Murphy, M.; et al. *Cell Metab.* **2016**, *23*, 379−385.

(10) Addanki, A.; Cahill, F. D.; Sotos, J. F. *J. Biol. Chem.* **1968**, *243*, 2337−2348.

(11) Gololobov, Y. G.; Kasukhin, L. F. *Tetrahedron* **1992**, *48*, 1353−1406.

(12) Saxon, E.; Bertozzi, C. R. *Science* **2000**, *287*, 2007−2010.

(13) Prescher, J. A.; Bertozzi, C. R. *Nat. Chem. Biol.* **2005**, *1*, 13−21.

(14) Sundhoro, M.; Jeon, S.; Park, J.; Ramstrom, O.; Yan, M. *Angew. Chem., Int. Ed.* **2017**, *56*, 12117−12121.

(15) Wada, T.; Ohkubo, A.; Mochizuki, A.; Sekine, S. *Tetrahedron Lett.* **2001**, *42*, 1069−1072.

(16) Wu, Z.; Li, Z.; Yang, L.; Han, J.; Han, S. *Chem. Commun.* **2012**, *48*, 10120−10122.

(17) Asin-Cayuela, J.; Manas, A. R.; James, A. M.; Smith, R. A.; Murphy, M. P. *FEBS Lett.* **2004**, *571*, 9−16.

(18) Kelso, G. F.; Porteous, C. M.; Coulter, C. V.; Hughes, G.; Porteous, W. K.; Ledgerwood, E. C.; Smith, R. A.; Murphy, M. P. *J. Biol. Chem.* **2001**, *276*, 4588−4596.

(19) Yuan, H.; Cho, H.; Chen, H. H.; Panagia, M.; Sosnovik, D. E.; Josephson, L. *Chem. Commun.* **2013**, *49*, 10361−10363.

(20) Heytler, P. G. *Biochemistry* **1963**, *2*, 357−361.

(21) Parker, V. H. *Nature* **1956**, *178*, 261.

(22) Xue, Z.; ZHao, H.; Liu, J.; Han, J.; Han, S. *Chem. Sci.* **2017**, *8*, 1915−1921.

(23) Xue, Z.; Zhao, H.; Liu, J.; Han, J.; Han, S. *Anal. Chem.* **2017**, *89*, 7795−7801.

(24) Wang, B.; Zhang, X.; Wang, C.; Chen, L.; Xiao, Y.; Pang, Y. *Analyst* **2015**, *140*, 5488−5494.

(25) Ren, W.; Ji, A.; Karmach, O.; Carter, D. G.; Martins-Green, M. M.; Ai, H. W. *Analyst* **2016**, *141*, 3679−3685.

(26) Tomas-Gamasa, M.; Martinez-Calvo, M.; Couceiro, J. R.; Mascarenas, J. L. *Nat. Commun.* **2016**, *7*, 12538.

(27) Chalmers, S.; Caldwell, S. T.; Quin, C.; Prime, T. A.; James, A. M.; Cairns, A. G.; Murphy, M. P.; McCarron, J. G.; Hartley, R. C. *J. Am. Chem. Soc.* **2012**, *134*, 758−761.

(28) Frank, M.; Duvezin-Caubet, S.; Koob, S.; Occhipinti, A.; Jagasia, R.; Petcherski, A.; Ruonala, M. O.; Priault, M.; Salin, B.; Reichert, A. S. *Biochim. Biophys. Acta, Mol. Cell Res.* **2012**, *1823*, 2297−2310.

(29) Heytler, P. G.; Prichard, W. W. *Biochem. Biophys. Res. Commun.* **1962**, *7*, 272−275.

(30) Pumphrey, A. M.; Redfearn, E. R. *Biochem. Biophys. Res. Commun.* **1962**, *8*, 92−96.

(31) Parker, W. D., Jr.; Oley, C. A.; Parks, J. K. *N. Engl. J. Med.* **1989**, *320*, 1331−1333.

(32) Nobes, C. D.; Brown, G. C.; Olive, P. N.; Brand, M. D. *J. Biol. Chem.* **1990**, *265*, 12903−12909.

(33) Trnka, J.; Blaikie, F. H.; Smith, R. A.; Murphy, M. P. *Free Radical Biol. Med.* **2008**, *44*, 1406−1419.

(34) Ward, M. W.; Rego, A. C.; Frenguelli, B. G.; Nicholls, D. G. J. *Neurosci.* **2000**, *20*, 7208−7219.

(35) Fulda, S.; Galluzzi, L.; Kroemer, G. *Nat. Rev. Drug Discovery* **2010**, *9*, 447−464.

(36) Pereira, P. M.; Silva, S.; Bispo, M.; Zuzarte, M.; Gomes, C.; Girao, H.; Cavaleiro, J. A.; Ribeiro, C. A.; Tome, J. P.; Fernandes, R. *Bioconjugate Chem.* **2016**, *27*, 2762−2769.

(37) Bar-Peled, L.; Sabatini, D. M. *Trends Cell Biol.* **2014**, *24*, 400−406.

(38) Lv, W.; Zhang, Z.; Zhang, K. Y.; Yang, H.; Liu, S.; Xu, A.; Guo, S.; Zhao, Q.; Huang, W. *Angew. Chem., Int. Ed.* **2016**, *55*, 9947−9951.

(39) Jung, H. S.; Lee, J. H.; Kim, K.; Koo, S.; Verwilst, P.; Sessler, J. L.; Kang, C.; Kim, J. S. *J. Am. Chem. Soc.* **2017**, *139*, 9972−9978.

(40) Chakrabortty, S.; Agrawalla, B. K.; Stumper, A.; Vegi, N. M.; Fischer, S.; Reichardt, C.; Kogler, M.; Dietzek, B.; Feuring-Buske, M.; Buske, C.; Rau, S.; Weil, T. *J. Am. Chem. Soc.* **2017**, *139*, 2512−2519.

(41) Zhang, C. J.; Hu, Q.; Feng, G.; Zhang, R.; Yuan, Y.; Lu, X.; Liu, B. *Chem. Sci.* **2015**, *6*, 4580−4586.